AD-A152 294 THE REMOTE DETECTION OF POLYNUCLEAR AROMATIC HYDROCARBONS USING LASER-INDUCED FLUORESCENCE(U) NAVAL WEAPONS CENTER CHINA LAKE CA R T LODA JAN 85 1/1

UNCLASSIFIED NWC-TP-6587 SBI-AD-E900 445 F/G 19/1 NL

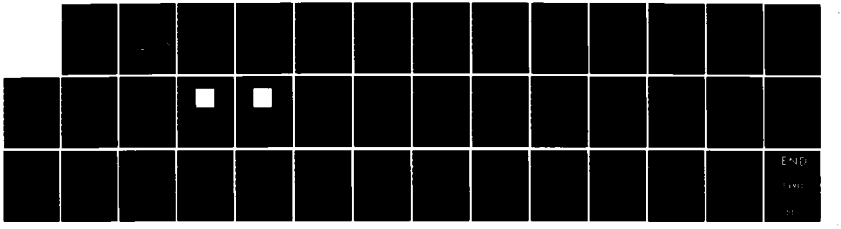

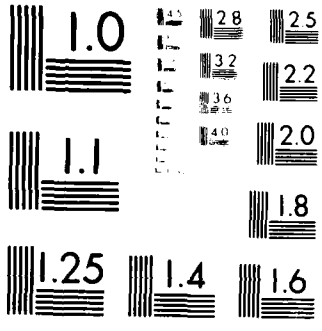

NWC TP 6587

(2)

The Remote Detection of Polynuclear Aromatic Hydrocarbons Using Laser-Induced Fluorescence

by
Richard T. Loda
Research Department

JANUARY 1985

NAVAL WEAPONS CENTER
CHINA LAKE, CA 93555-6001

Naval Weapons Center
AN ACTIVITY OF THE NAVAL MATERIAL COMMAND

FOREWORD

Polynuclear aromatic hydrocarbons (PAHs) can be produced during the thermal destruction (demilitarization) of unserviceable propellant, explosive, and pyrotechnic (PEP) materials. Because some of these PAH compounds are carcinogenic, there is a need to monitor their possible release into the environment. The feasibility of using laser-based techniques for the real-time, remote detection of atmospheric PAHs during the large-scale incineration of PEP materials is the subject of this report.

The work described herein took place from January 1982 to August 1984. The work was performed under the sponsorship of G. Young of the Naval Surface Weapons Center, White Oak Laboratory, Silver Spring, Md. (Task S0400, Element Number 63721N, and Work Unit 138567), and J. Short of the Naval Weapons Support Center, Crane, Ind. (Task SF65559, Element Number 62765N, and Work Unit 138568).

This work has been reviewed for technical accuracy by D. A. Fine and T. P. Parr.

Approved by
E. B. ROYCE, Head
Research Department
15 November 1984

Under authority of
K. A. DICKERSON
Capt., U.S. Navy
Commander

Released for publication by
B. W. HAYS
Technical Director

NWC Technical Publication 6587

Published by . . . . . Technical Information Department
Collation . . . . . Cover, 18 leaves
First printing . . . . . 150 copies

UNCLASSIFIED

SECURITY CLASSIFICATION OF THIS PAGE (When Data Entered)

REPORT DOCUMENTATION PAGE		READ INSTRUCTIONS BEFORE COMPLETING FORM
1. REPORT NUMBER NWC TP 6587	2. GOVT ACCESSION NO. AD-A152 294	3. RECIPIENT'S CATALOG NUMBER
4. TITLE (and Subtitle) THE REMOTE DETECTION OF POLYNUCLEAR AROMATIC HYDROCARBONS USING LASER-INDUCED FLUORESCENCE		5. TYPE OF REPORT & PERIOD COVERED Interim January 1982-August 1984
		6. PERFORMING ORG. REPORT NUMBER
7. AUTHOR(s) Richard T. Loda		8. CONTRACT OR GRANT NUMBER(s)
9. PERFORMING ORGANIZATION NAME AND ADDRESS Naval Weapons Center China Lake, CA 93555-6001		10. PROGRAM ELEMENT, PROJECT, TASK AREA & WORK UNIT NUMBERS PE 63721N & 62765N, Task S0400 & SF65559, Work Unit 138567 & 138568
11. CONTROLLING OFFICE NAME AND ADDRESS Naval Weapons Center China Lake, CA 93555-6001		12. REPORT DATE January 1985
		13. NUMBER OF PAGES 34
14. MONITORING AGENCY NAME & ADDRESS(if different from Controlling Office)		15. SECURITY CLASS. (of this report) UNCLASSIFIED
		15a. DECLASSIFICATION/DOWNGRADING SCHEDULE

16. DISTRIBUTION STATEMENT (of this Report)

Approved for public release; distribution is unlimited.

17. DISTRIBUTION STATEMENT (of the abstract entered in Block 20, if different from Report)

18. SUPPLEMENTARY NOTES

19. KEY WORDS (Continue on reverse side if necessary and identify by block number)

Explosives
Gas-phase
Laser-induced fluorescence
Polynuclear aromatic hydrocarbons
Propellants
Pyrotechnics
Remote detection

20. ABSTRACT (Continue on reverse side if necessary and identify by block number)

See back of form.

DD FORM 1 JAN 73 1473 EDITION OF 1 NOV 65 IS OBSOLETE
S/N 0102-LF-014-6601

UNCLASSIFIED

SECURITY CLASSIFICATION OF THIS PAGE (When Data Entered)

(U) The Remote Detection of Polynuclear Aromatic Hydrocarbons Using Laser-Induced Fluorescence, by Richard T. Loda, China Lake, Calif., Naval Weapons Center, January 1985, 34 pp. (NWC TP 6587, publication UNCLASSIFIED).

(U) This publication discusses the feasibility of remotely detecting gas-phase polynuclear aromatic hydrocarbons (PAHs) that might be produced during the combustion of propellant, explosive, and pyrotechnic (PEP) materials. Laboratory scale and remote laser-induced fluorescence measurements are presented. Projections, based on measured gas- to solution-phase sensitivity factors and reasonable system improvements, indicate that 1 ppm concentration levels could be detected, at a range of approximately 1 km. The complex selectivity problems associated with the analysis of multicomponent mixtures are discussed, and some remote sensing system component recommendations are also given.

CONTENTS

ACKNOWLEDGEMENTS

The author would like to thank Timothy Parr (NWC, Code 3893) for many valuable discussions, in addition to his assistance with both experimental work and equipment, during the remote sensing studies.

INTRODUCTION

Large-scale smoky burns of propellant, explosive, and pyrotechnic (PEP) materials at Naval establishments can lead to complaints from neighbors and air pollution boards. It is often difficult and dangerous to transport such materials to bases where nonpolluting demilitarization is possible. Collecting and analyzing representative samples from large burns for environmentally hazardous materials has proven to be a difficult and costly engineering problem. It has been done for only a few such samples to date.

A number of laser-based analytical techniques have been developed for the purposes of direct atmospheric monitoring. This report discusses the feasibility of using laser-based analytical methods to remotely monitor the atmosphere for polynuclear aromatic hydrocarbons (PAHs) which may be produced during the large-scale combustion of PEP materials. Since some of these PAHs are carcinogenic, effective monitoring and control of PAH emissions from these burns must be achieved for this demilitarization process to be deemed fully acceptable.

Initial work on this pollution abatement project began with the design, construction, and operation of a real-time incinerator stack gas monitor for the Naval Weapons Support Center (NWSC), Crane, Indiana. This sub-task was felt to be simpler than, but strongly related to, the more complicated remote sensing requirement necessary for the larger PEP burns. The incinerator monitor was also a more immediate need. Two reports have been published on this earlier work (References 1 and 2) and much of the information presented here is relevant to the remote sensing problem.

Because of the reprogramming of pollution abatement funds in fiscal year 1984, this report emphasizes analysis and feasibility, rather than the design and operation of a specific remote sensing instrument. Background material specific to the remote sensing and PAH detection problem will be discussed first. Following this, experimental details will be given for the work described here. The results of some laboratory scale and remote laser-induced fluorescence experiments will be covered next. This will be followed by some detection level projections for an improved system and a discussion of the problems associated with selective identification in a multicomponent mixture environment. Finally, some component recommendations for a laser-based remote PAH monitor will be given.

BACKGROUND

The incomplete combustion of hydrocarbons can result in the production of hazardous PAH materials. Without proper controls, these chemicals can then be released into the environment and contribute to overall global pollution. It is known that PAHs have been produced during the large-scale combustion and/or detonation of PEP materials (References 1 through 12). There is an obvious need to monitor these processes in real-time to determine the full extent of the problem. Safety requirements would demand the use of remote sensing techniques during this monitoring operation.

Remote sensing can be defined as the qualitative and/or quantitative monitoring of a chemical or physical parameter in the environment where the monitoring instrument and the parameter under investigation are spatially separated. This field has been the subject of numerous publications (References 13 through 16). Atmospheric monitoring is largely based on applied atomic and molecular spectroscopy. The interaction between electromagnetic radiation and atoms and molecules serves as the basis for detecting and continuously monitoring atmospheric constituents and properties. Remote sensing has become increasingly important for pollution detection because it provides a number of advantages over standard single-point sampling techniques. It is not meant to be a substitute for *in situ* point-sampling, but considered to be an adjunct to it. However, in cases such as the incineration of hazardous (i.e., toxic, explosive) PEP materials, remote sensing probably represents the only economical or technically feasible way to approach the pollution monitoring problem. Some of the unique features of remote sensing are listed below:

1. Nonintrusive measurements are possible. No extraction of source gases is required. Therefore, the possibility of modifying the sample during the measurement process is eliminated. This point is important because sample recovery and the maintenance of sample integrity during the workup prior to analysis is known to be a serious problem for the PAHs (References 17 and 18). Also, measurements can be made without shutting down the facility under investigation. This can be done unannounced and from a location off of the property (surveillance).

2. Integrated-path measurements are possible with remote techniques. This permits a more accurate estimation of the total pollutant concentration than that obtained with point-sampling methods.

3. Three-dimensional measurements are possible. Historically, air pollution monitoring has been performed using wet chemical techniques and grab sampling for later laboratory analysis. In general, these methods are limited to making single-point measurements. A

single remote sensing instrument has the capability of making measurements over a variety of locations, both at ground level and aloft. It can also be used to survey possible locations for *in situ* monitors.

4. Measurements are possible over large geographical areas with instrumentation mounted on trucks, aircraft, etc.

In the remote sensing of pollutants, information can be obtained through spatial, spectral, and temporal resolution. Basic techniques can be divided into two broad categories: active and passive. The difference between these two categories depends upon the source of the electromagnetic radiation employed. Passive techniques make use of the existing radiation in the atmosphere (e.g., solar and earth-reflected or emitted radiation). The interaction of this radiation with the species under investigation or the thermal emission of this species is observed to infer concentration. Active techniques introduce specific radiation into the atmosphere. Typically, lasers are used as the source of this radiation. As with the passive category, the interaction of this laser radiation with the species under investigation is then observed to infer concentration. Active techniques can be further subdivided into single-ended and double-ended systems. Single-ended systems colocate the laser source and the receiver. Double-ended systems either have the laser and receiver located separately, or have them co-located, with a physical reflector located at a distance. The emphasis will be placed on active remote sensing techniques for the rest of our discussion. We expect that this category will be the most useful in the remote detection of PAHs in PEP burns.

Some examples of active remote sensing techniques include light, detection and ranging, or laser radar (LIDAR) (References 13 through 16), Raman LIDAR (References 13 through 19), differential absorption LIDAR (DIAL) (References 19 through 22), resonance LIDAR (Reference 13), and molecular fluorescence LIDAR (References 19 and 23 through 29). Fundamentally, LIDAR systems consist of a laser source and a telescope to observe the scattered radiation. The optical field-of-view of the telescope includes the laser beam as it propagates through the atmosphere. The selection of the laser wavelength, the receiver wavelength, and the data analysis and interpretation delineate the key differences between all the LIDAR-based techniques mentioned above.

For the basic LIDAR system, the detector wavelength is matched to the laser wavelength. The detected signal is recorded as a function of time, thus providing a range-resolved measure of atmospheric scattering. This technique is of limited use for our present problem.

In Raman LIDAR, the receiver wavelength is shifted to a value which corresponds to the specific Raman shift for the atmospheric species to be monitored. The magnitude of the shift is unique to the particular

scattering molecule, and the intensity observed is proportional to its concentration. The greatest drawback to this technique comes from the fact that most molecules have low cross sections for Raman scattering. Therefore, its utility is limited to cases where high molecular concentrations are present. With regard to the specific PAH monitoring problem we are concerned with here, it is also quite likely that any Raman scattering that might be present would be swamped by PAH fluorescence (References 1, 2, 13, 14, and 19). This would preclude its use as a PAH detection technique.

In DIAL the laser beam is alternately tuned on and off resonance with an absorption band of the pollutant molecule. The return signal is obtained from atmospheric aerosol and particulate scattering, i.e., the atmosphere is used as a distributed retroreflector, and the time resolved backscattered intensity is recorded. The concentration of the pollutant molecule can be calculated from a knowledge of the difference between the absorption cross sections at the two measurement wavelengths. The high cross sections for absorption (relative to Raman, for example) (References 13, 14, and 19) make DIAL the most sensitive of the current LIDAR techniques. However, DIAL is not without its disadvantages. In the analysis, the aerosol, particulate and molecular scattering parameters are assumed to be equal at the on and off resonance laser wavelengths. This assumption is valid only when the beams are spectrally separated by a small wavelength increment. The technique is thus principally used to investigate simple diatomic and triatomic molecules that have highly resolved absorption spectra. This is not the case for the more complicated PAH molecules, which have absorption features with bandwidths on the order of tens of nanometers, even in the gas phase (References 1, 2, 26, and 28). Another complication arises if there is an interfering gas which does not have the same absorption cross section at both laser wavelengths. The concentration and absorption cross section of the interfering gas must be known, or determined by a separate experiment. For complex mixtures of PAHs in a smoke plume, the number of laser probe wavelengths required for analysis is at least one more than the number of significant molecular absorbers. Regarding this last point, it should be emphasized that the PAHs are not likely to be the only significant molecular absorbers in the plume. It is important to realize that a great deal of laboratory spectroscopy is necessary before these LIDAR-based systems can be used for the remote sensing of pollutants. Accurate spectral data on both the pollutant of interest and all interfering species should be collected in order to interpret results correctly. Because of the problems mentioned above, it is unlikely that DIAL would be the most useful technique for PAH detection.

In resonance LIDAR, both the laser and receiver wavelengths are matched to an absorption wavelength of the pollutant species. The resonant scattering produced is significantly more intense than nonresonant scattering. This technique has been successfully used for atomic detection. Unfortunately, resonance scattering cross section

values for molecules are much smaller than the corresponding values for atoms (References 13 and 19). This is because the re-emission for molecules is distributed among the more closely spaced energy levels of the molecules (compared to atoms) and because only a small fraction of the molecules populate any particular initial level. Radiationless quenching in the lower atmosphere also reduces the signal level in resonance LIDAR. Although the atmospheric quenching problem is not severe for PAHs (Reference 1), the interfering gas and PAH mixture complexity issues mentioned in the previous paragraph would seriously limit the utility of this technique for our present purposes.

In molecular fluorescence LIDAR, the laser wavelength is matched to an absorption wavelength of the pollutant molecule, but the receiver is set to observe the characteristic fluorescent emission of the pollutant at a wavelength, or set of wavelengths, other than that of the laser source. This technique has been used successfully to remotely monitor PAHs in solution and in oil spills (References 23 through 25, 27, and 29). The advantage of this LIDAR-based method, with regard to the remote detection of complex PAH mixtures, lies in the ability of the operator to choose two wavelengths (excitation and emission) for the measurement of the fluorescing species. This leads to an enhanced detection selectivity for the highly fluorescing PAHs, since not all absorbing molecules will fluoresce. This selectivity principle can also be used to discriminate between the different individual PAH molecules in the mixture.

In the references given in the previous paragraph, molecular fluorescence LIDAR has been used to detect PAH solutions, on an approximate part per million (ppm) scale, at a range of a few tens to a few hundred meters. Sub-ppm solution detection levels have also been estimated for "improved" LIDAR fluorosensing systems. Unfortunately, the emphasis thus far has either been on the detectability of a single PAH, or, in the case of the oil studies, on the generation of a "fingerprint" spectrum that allows the discrimination of a number of complex oil samples. Little, if any attempt has been made to identify and quantify PAH mixture components. Identification and quantification are the most complicated problems that one faces in trying to implement the remote detection of PAHs in PEP burns. Previously, 10 or more PAHs have been shown to be present during the combustion of PEPs (References 3 and 4). The overlap of the excitation and emission spectra for the different components and the inherently featureless nature of the individual spectra present real difficulties to the analyst. Nevertheless, sophisticated fluorescence-based techniques have been employed to improve standard multicomponent analyses (References 30 and 31) and a variety of numerical algorithms have been used to deconvolute overlapping spectra (References 32 and 33). Application of these procedures to remote sensing should help alleviate some of these expected difficulties.

There has been no reported gas-phase PAH remote detection work. One must realize that the potential sensitivity of the systems described above would be orders of magnitude less for gas-phase versus solution-phase PAH detection (Reference 2). This rough estimation is based on the change in density in going from the gas-phase to solution, and the effect of atmospheric quenching. Also, at lower temperatures in the PEP combustion smoke plume, most PAHs would be condensed onto particulate matter (References 34 through 38). This leads to a potential spectral complexity problem that is at least as great as that described in the previous paragraph. In the absence of any separation steps in the analytical procedure, workers have only been able to obtain "fingerprinted" spectra from different particulate sources. This fact is probably best exemplified by the statements of one group of authors:

> "It is obvious that the above experiments only paint in broad strokes what we may hope to learn by application of the fluorescence techniques to the study of fly ash emissions. Much detailed work is required to elucidate what the fluorescence can tell us about the makeup of the fly ash and what, specifically, in the fly ash produces the observed emissions and their intensities." (Reference 34.)

To simplify the analysis in this situation, spectral deconvolution techniques could also be applied.

EXPERIMENTAL

MATERIALS

Anthracene was purchased from Matheson, Coleman and Bell, East Rutherford, N.J., and was used without further purification after it was determined that its melting point was 216°C (Reference 39). Phenanthrene was purchased from Eastman Chemical Products, Inc., Kingsport, Tenn., and was recrystallized from ethanol until the melting point agreed with the literature value of 101°C (Reference 39). Baker reagent cyclohexane was used as received to prepare the PAH solutions.

LABORATORY FLUORIMETER

The Spex Instruments, Inc., Edison, N.J., FLUOROLOG 2 Fl12 fluorimeter has been described in great detail elsewhere (References 1 and 40). The sample heater/controller block (Reference 1) was installed for the measurements as a function of temperature. Quartz

cuvettes from NSG Precision Cells, Inc., Hicksville, N.Y., were used for sample containment. The optical pathlength of the cells was 1.0 cm. The static cell, gas-phase PAH fluorescence measurements were made by first placing a small amount of solid PAH in the bottom of a cuvette. The cuvette was then sealed with its Teflon stopper. The sample (PAH in air) was next placed in the fluorimeter sample compartment and allowed to equilibrate at the set-point temperature. The gas-phase fluorescence spectrum (or time dependent intensity scan) was then recorded for the wavelength range of interest. As an instrumental reference, background spectra were recorded under the same conditions using a cuvette containing only air.

Solution spectra were recorded at room temperature (22°C) using methods similar to those described above. Background spectra were recorded using pure cyclohexane. A stock solution of anthracene in cyclohexane was made by dissolving a small amount of anthracene in 250 mL of cyclohexane. The absorption spectrum of this solution was then taken on a Beckman DU-7 absorption spectrophotometer. Using the known absorption coefficient of anthracene in cyclohexane (Reference 41), the concentration of the solution was calculated to be 9.18×10^{-6} M (2.1 ppm). A second solution was prepared by diluting the stock solution by a factor of 500, giving a concentration of 1.84×10^{-8} M (4.2 parts per billion (ppb)).

All spectra were recorded using a right angle detection geometry, and the spectral resolution was approximately 5 nm for both the excitation and emission wavelengths. Wavelength scanning was done in a burst mode, at 1 nm/step, with a 1-second integration time. Intensity versus time plots at fixed excitation and emission wavelengths were taken using an integration time of 1 second.

LABORATORY LASER-INDUCED FLUORESCENCE (LIF) SYSTEM

The LIF system used for the laboratory scale experiments is diagrammed in Figure 1. A Lumonics TF 861T-3 rare gas halide excimer laser, operated on the XeCl line (308 nm), was used to pump a Lumonics EPD-330 dye laser. A 2-inch diameter CVI Corporation XC-2 dielectrically coated, >99% reflectivity 308 nm mirror was used to steer the excimer pump beam to the dye laser. The excimer operated with a pulse energy between 55-65 mJ in an 8-ns pulse during the experiments reported here. The pulse repetition frequency was normally 10 Hz. The laser dye was a 1×10^{-3} M solution of p-terphenyl in p-dioxane. This dye operated with a tuning range of 335-349 nm, and the bandwidth was nominally 0.26 cm^{-1}. The output power of the dye laser near 340 nm was approximately 1.8 mJ in a 6-ns pulse. The full-angle beam divergence was roughly 1 mrad.

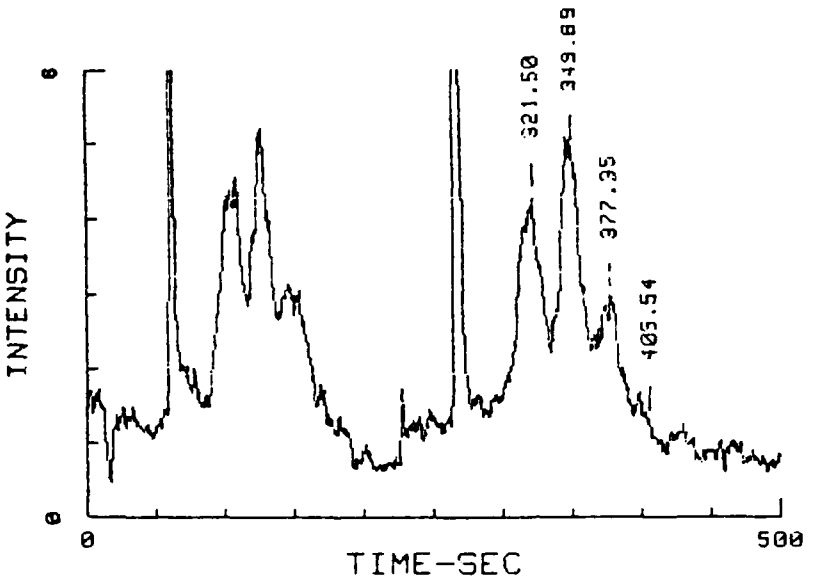

FIGURE 12. Two Successive Remote LIF Emission Spectra of the 2.1 ppm Solution of Anthracene in Cyclohexane. The sample location was 63 m from the receiver telescope and the excitation wavelength was 340 nm. The boxcar settings were as in Figure 11 and the emission wavelengths of 380, 400, 420, and 450 nm occurred at 321, 349, 377 and 405 seconds.

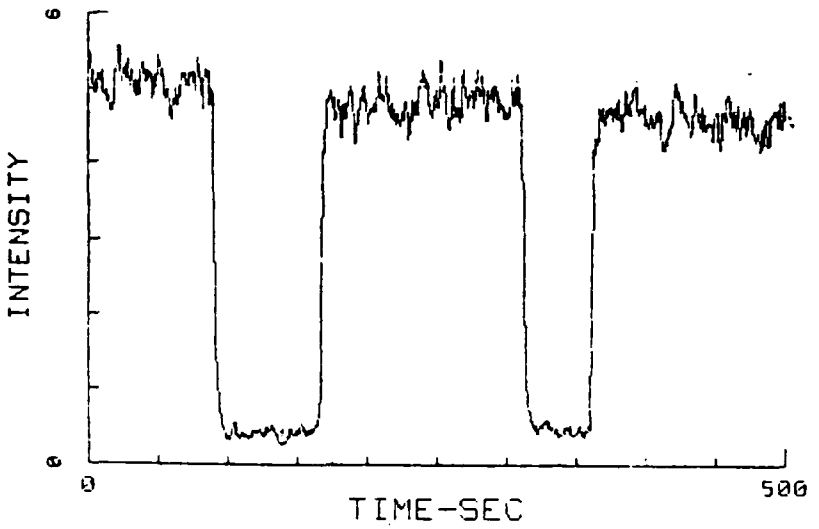

FIGURE 11. Remote LIF Intensity Versus Time Plot for the 2.1 ppm Solution of Anthracene in Cyclohexane. The sample location was 63 *m* from the receiver telescope. The excitation and emission wavelengths were 340 nm and 400 nm, respectively. The boxcar was terminated at 1 megohm, the gate time was 0.5 μs, and the aperture delay was 3.2 μs. The square-wave nature of the plot was produced by the removal and reinsertion of the sample cell. More than 50% of the background level was caused by the LIF of the black posterboard at the sample location.

modified by absorption in the atmosphere (References 14 and 15). The maximum of solar irradiance occurs in the visible region of the spectrum and this radiation strongly overlaps the LIF emission from PAHs. This background contribution would be especially detrimental if it were necessary to operate the remote sensing system under full daylight conditions. In this case, 50 Ω termination and short gate times would enable the temporal discrimination of this unwanted background (References 23 through 25 and 27).

The remote LIF emission spectrum of the solution of 2.1 ppm anthracene in cyclohexane taken under 50 Ω termination conditions, is given in Figure 14. The reduced baseline in this experiment, compared to that obtained with 1 mΩ termination, was brought about by the temporal discrimination against the longer-lived black posterboard LIF.

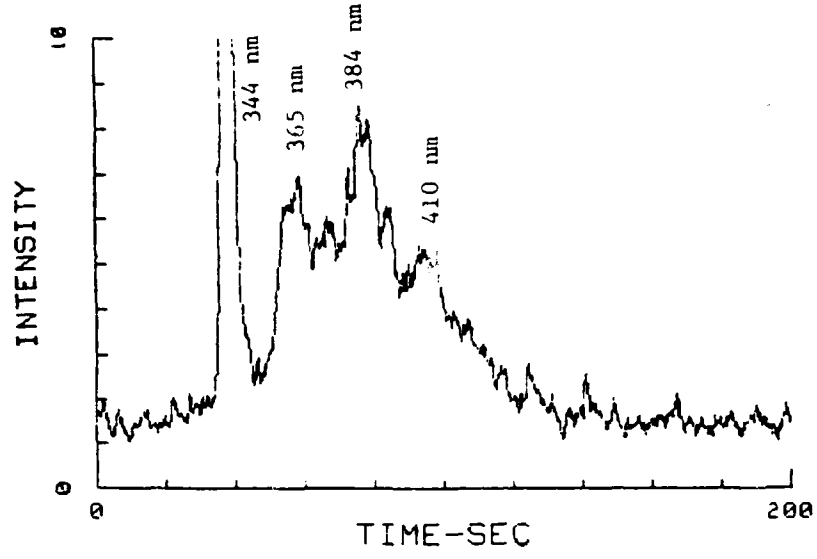

FIGURE 9. LIF Emission Spectrum of the Anthracene in Air Sample. The temperature was 23°C, and the excitation wavelength was 344 nm. The first intense peak was produced by laser scatter at 344 nm. The three predominant anthracene peaks occurred at 365, 384, and 410 nm. This emission was saturated.

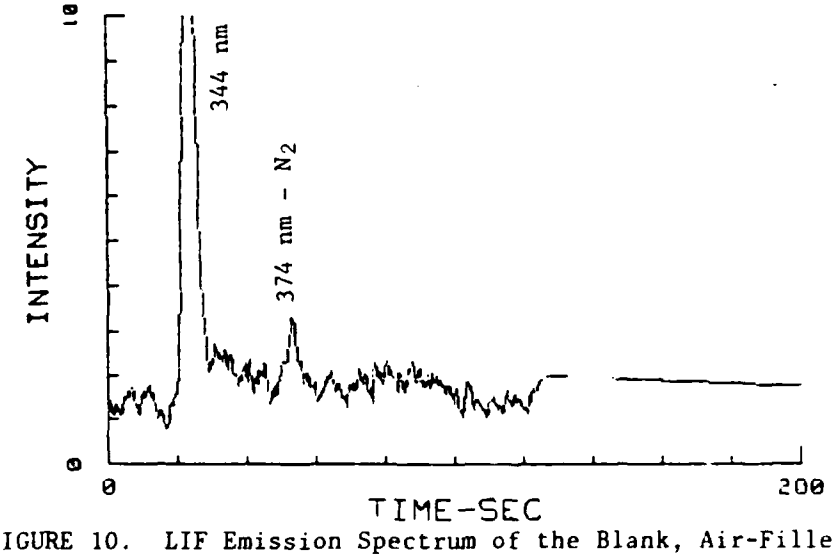

FIGURE 10. LIF Emission Spectrum of the Blank, Air-Filled Sample Cell. The temperature was 23°C, and the excitation wavelength was 344 nm. The first intense peak was produced by laser scatter at 344 nm. The weak feature is at 374 nm which corresponds to the nitrogen Raman shift of 2331 cm^{-1} (References 13 and 19). Data collection was terminated at 125 seconds.

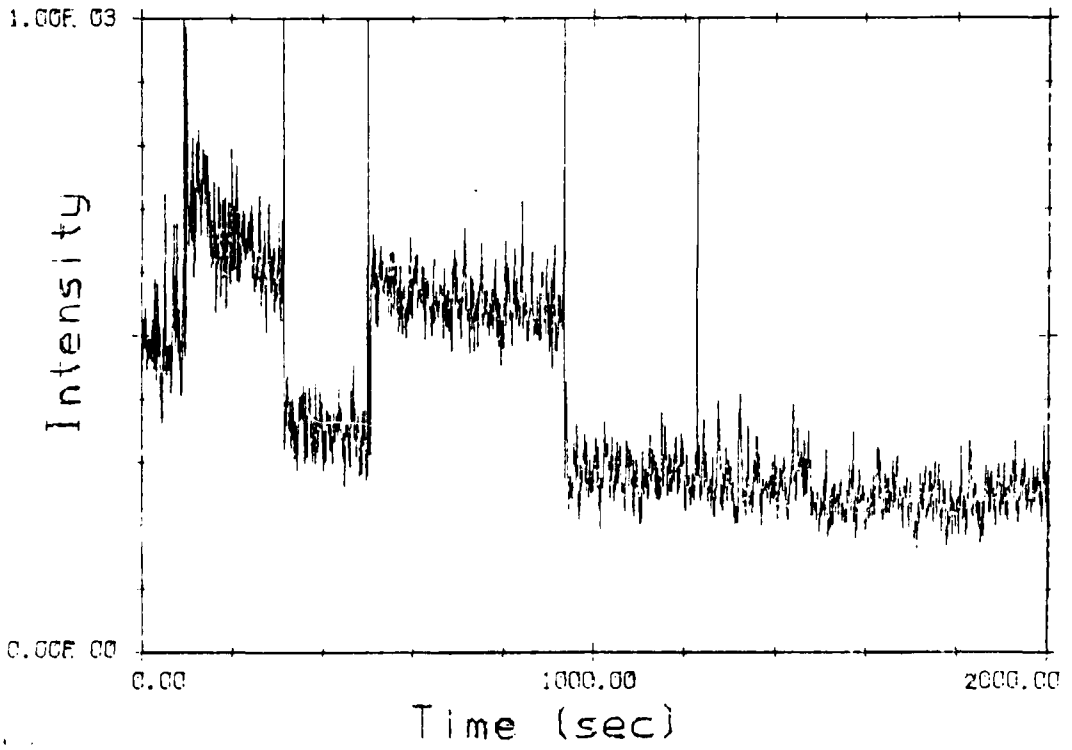

FIGURE 8. Anthracene in Air Fluorescence Intensity Versus Time Plot Taken on the Spex Fluorimeter. The temperature was 21.1°C and the excitation and emission wavelengths were 344 nm and 384 nm, respectively. The square-wave nature of the plot was produced by swapping the sample and blank cells while the plot was in progress.

reminded that the fluorescence observed in the gas-phase LIF was saturated. Such was not the case for this remote solution-phase study. Since Raman signals do not saturate, one would expect that the Raman contribution to the total emission would be greater under saturated conditions as was observed.

When the boxcar averager is terminated at 1 mΩ, the receiving system is essentially useless for ranging information. This is because the RC time constant may be on the order of hundreds of microseconds. One hundred microseconds would correspond to a range resolution of 1.5×10^4 m (References 13 and 19). Another disadvantage of this experimental arrangement is that more noise and background scatter are integrated with the signal when long gate times are used. The sun radiates essentially as a Planck radiator of temperature 6000 K but

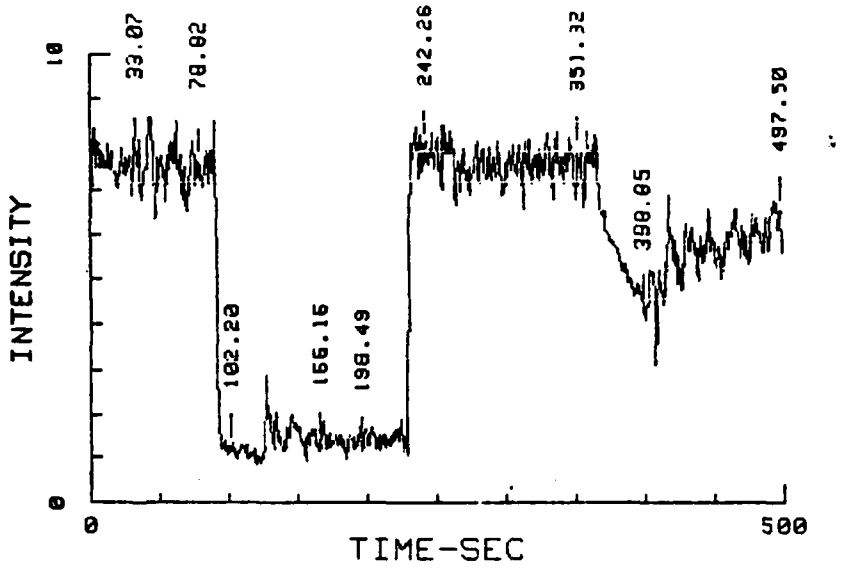

FIGURE 7. Anthracene in Air LIF Intensity Versus Time Plot. The temperature was 23°C. The excitation wavelength was 344 nm and the emission wavelength was 384 nm. The decrease in intensity at 90 seconds was caused by the removal of sample cell. A blank cell was inserted at 125 seconds and the sample cell re-inserted at 230 seconds. The pulse repetition frequency of the laser was increased from 10 to 100 Hz at 360 seconds. The decrease in signal at the point was caused by the decreased pulse energy at the higher repetition frequency. The pulse repetition frequency was decreased from 100 to 10 Hz at 400 seconds.

REMOTE LIF EXPERIMENTS

A remote LIF intensity versus time plot for the 2.1 ppm solution of anthracene in cyclohexane is given in Figure 11, and two successive remote LIF emission spectra are presented in Figure 12. These data are in excellent agreement with the fluorescence emission spectrum of anthracene in cyclohexane given in the literature (Reference 41). The remote response to a pure cyclohexane blank is shown in Figure 13. It was anticipated that the strongest solvent Raman transition at 378 nm (2950 cm^{-1} shift) would be observed during this experiment, but as can be seen from the figure, it was not. This was initially surprising given the results in Figures 9 and 10, but the reader should be

The fluorescence emission spectrum of the 4.2 ppb solution of anthracene in cyclohexane was next measured using an excitation wavelength of 357 nm. The maximum emission intensity was found to be 6.23×10^5 counts at 378 nm (after subtracting the solvent Raman contributions). The solution-phase detection sensitivity was calculated to be 1.48×10^8 counts/ppm for anthracene in cyclohexane. At 50°C the extrapolated vapor pressure is 1.457×10^{-4} torr (Reference 42) which results in a calculated anthracene concentration of 208 ppb. The measured fluorescence intensity value was 5.2×10^4 counts, from which it follows that the gas-phase (air) detection sensitivity of anthracene was 2.5×10^5 counts/ppm. Therefore, the gas- to solution-phase sensitivity factor is 592, which agrees reasonably well with the expected density change of about 700. A higher factor had been anticipated, based on the atmospheric quenching known to occur in the gas-phase (References 1 and 2), but other workers have found that gas-phase fluorescence quantum yields for aromatic hydrocarbons are not greatly different from their solution-phase values, and that these yields may increase or decrease as a function of temperature, depending on the individual molecule (References 43 through 45). Nonetheless, this measurement will be used as a "representative" value later in this report.

LABORATORY LIF EXPERIMENTS

A LIF intensity versus time plot for anthracene in air is presented in Figure 7, which can be compared to the fluorimeter data given in Figure 8. Using the literature value for the anthracene vapor pressure at 50°C (Reference 42) and extrapolating the fluorescence intensity data (Figure 6) to approximately 22°C, the anthracene concentration was calculated to be on the order of 1 ppb. As expected, there was an increase in signal to noise for the LIF measurement relative to the fluorimeter results, and these detection sensitivity levels compare quite favorably to other work (Reference 46), especially when one considers that our results were obtained in ambient air.

Figures 9 and 10 show plots of fluorescence emission intensity versus wavelength for the anthracene in air sample and the blank cell. The monochromator was manually scanned during the real-time data acquisition. The emission spectrum of Figure 9 is in excellent agreement with previously measured gas-phase anthracene spectra (Reference 1), and the weak feature in Figure 10 is actually the Raman signal from N_2 present in the room air within the blank cell. It should be mentioned that with the laser power level used here, the anthracene emission was saturated. This does not affect the detectability level, but it would make the fluorescence intensity as a function of laser fluence nonlinear. This is not important for our present purposes and also will not be a problem in the remote sensing work because of the reduced laser power density level at the remote sample location.

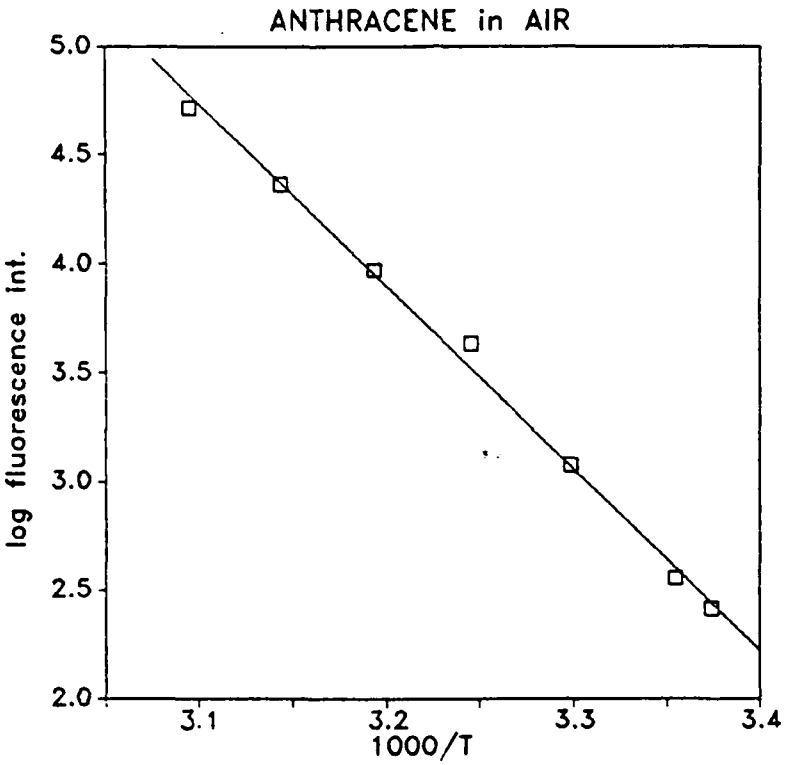

FIGURE 6. Plot of Air Fluorescence Intensity Versus 1000/T (in °K) for Anthracene in Air. The squares are the measured data points and the line represents the least squares fit to $\log_{10} I = 8361.9/T+30.657$. The correlation coefficient of the fit was 0.9977.

set-point range of the heater/controller block. It was concluded that the most accurate data to use for the gas-phase sensitivity determination was the 50°C fluorescence intensity data and the vapor pressure calculated from the 65.7 to 80.4°C extrapolation (Reference 42). Anthracene vapor pressures (concentrations) at lower temperatures would be extrapolated from the fluorescence intensity measurements. As a final point concerning this issue, it should be noted that in a previous publication (Reference 1) the vapor pressure value at 50°C (and hence the concentration for a fluorescence experiment) was extrapolated from data taken over the 100 to 600°C range (Reference 39). Given the present findings, the concentration value should have been a maximum of 249 ppb, rather than the 3.6 ppm value quoted in the text. This fact does not change any of the major findings of the previous report, but means that the PAH monitor detection sensitivity to anthracene was greater than first proposed.

differences were observed. Also, the signal intensity for the room-temperature measurement, taken after the temperature cycling, was the same as that obtained originally.

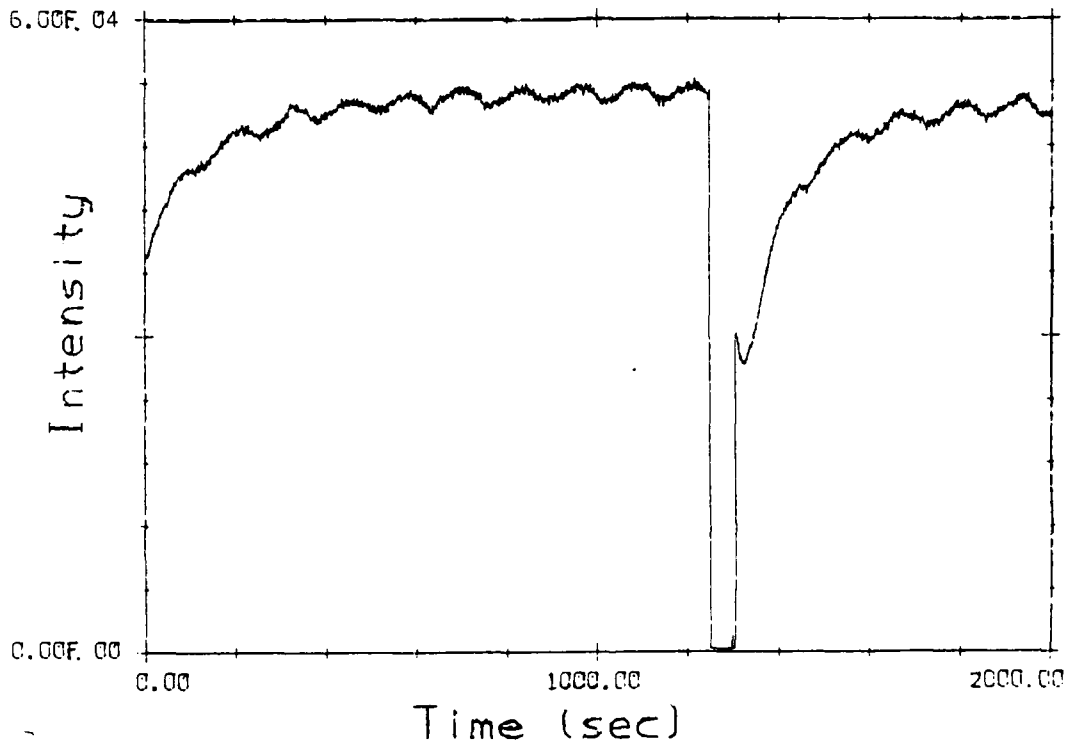

FIGURE 5. Anthracene in Air Fluorescence Intensity Versus Time Plot Taken at 50°C. The excitation wavelength was 344 nm and the emission wavelength was 384 nm. The reduction of the signal at 1250 seconds was caused by the insertion of the blank cell. The slow oscillations in the signal were caused by the temperature fluctuations during the on/off cycle of the cell block temperature controller.

To check our suspicions further, the fluorescence of phenanthrene in air was next examined, over a temperature range from 36.7 to 49.65°C. For this compound, there was only a 37% discrepancy between the fluorescence intensity measurements and the interpolated vapor pressure values (Reference 42). This result should be compared to the 576% discrepancy in the anthracene best-case extrapolation, and it should be emphasized that about half of the phenanthrene error can be explained by considering the absolute accuracy of the set-point and

proportional to its concentration. Gas-phase (air) PAH concentrations can also be calculated using the following expression:

$$ppm = (p/P) \times 10^6 \quad (1)$$

where

ppm = parts per million
p = partial pressure of PAH vapor
P = total gas pressure (700 torr for NWC)

This equation and the above facts provide a simple way to relate fluorescence intensity and sample concentration values.

In some preliminary fluorescence intensity measurements on gas-phase anthracene, it was noticed that for certain temperature ranges the intensity changed more dramatically than the extrapolated* vapor pressure changed. For example, from literature data (Reference 39) taken over 100 to 600°C, the vapor pressure was extrapolated to increase by a factor of 9 over the temperature range from 25 to 50°C. The fluorescence intensity was observed to change by a factor of 144 over this same temperature range. Using other literature data (Reference 42) taken from 65.7 to 80.4°C, the extrapolated vapor pressure change for the 25 to 50°C range was calculated to be 25. This is still a significant discrepancy, even though the extrapolation was only performed over 30 to 40°C. Because these findings directly affect the gas- to solution-phase detection sensitivity factor accuracy, a more detailed examination was deemed necessary.

Fluorescence intensity measurements were made for an anthracene/air sample at 5°C intervals over the range from 25 to 50°C. A representative intensity versus time plot, taken at 50°C, is shown in Figure 5. These data, and data taken at the other temperatures, were fitted to a straight line of the form $\log_{10} I = a/T + b$ (see Figure 6). These results are just the kind of behavior one would expect for the vapor pressure (concentration) and lead one to question the extrapolated vapor pressure values discussed above. In a static cell, once the cell has been heated and then cooled back to room temperature, solid PAH could condense on the cell walls. This would subsequently cause erroneous measured fluorescence intensities. However, it was felt that this was not the case here because solid anthracene has different excitation and emission spectra than gas-phase anthracene and no

*Literature vapor pressure data were fit to an equation of the form $\log_{10} P = a/T + b$ to determine values for a and b. With these values vapor pressure (P) could then be calculated at another temperature (T).

FIGURE 4. Sample Cell (7.5 cm diameter) Taped Onto the Black Posterboard Background.

RESULTS AND DISCUSSION

PRELIMINARY CONSIDERATIONS

The basic experimental approach used for this PAH remote detection feasibility study was as follows. First, gas- and solution-phase fluorescence intensity measurements would be compared for a representative PAH. Since this relative sensitivity value would be instrument independent, these experiments could be done most conveniently using the laboratory fluorimeter system. Next, PAH LIF experiments would be conducted on a laboratory scale, as a lead-in to the remote sensing investigations. Finally, remote LIF experiments would be performed on a representative PAH solution, and an extrapolation would be made to predict gas-phase remote detection levels. These experiments will be described in greater detail in the following sections.

FLUORIMETER EXPERIMENTS

If one excludes the presence of interfering species and non-linear effects,* the fluorescence intensity emitted from a sample is directly

*Non-linear effects are only applicable when intense excitation sources such as lasers are used.

FIGURE 3. Receiver Components of the Remote LIF System. The final laser beam-steering mirror can be seen just to the right of the telescope.

The samples were contained in two 7.5 cm diameter, 0.5 cm pathlength quartz cells (Figure 4). The 2.1 ppm solution of anthracene in cyclohexane was put in one cell, and the other was filled with cyclohexane. Black posterboard was mounted on the wall at the sample location, 63 m from the telescope. The two cells were alternately taped onto the posterboard during the experiments. The dye laser beam overfilled the sample cells at their location. During the initial alignment, the brightest part of the beam was adjusted to maximally overlap the sample. Although it is difficult to make an estimate without more careful experimentation, it is likely that at least 40% of the beam energy was not directly illuminating the sample. This would mean that the pulse energy at the sample was on the order of 1 mJ (neglecting any atmospheric losses).

The remote sensing experiments were performed at night, and for eye safety the doors at the end of the hallway were closed and covered with posterboard. The main hallway lights were turned off, but no attempt was made to shield the instrumentation from the hallway fire-safety lights or the ambient light coming from the electronic instrumentation and computer screen. A weak flashlight was used near the monochromator/photomultiplier while the experiments were in progress to allow the operator to read and record the monochromator wavelengths.

The returning Molecular Fluorescence LIDAR signals were received by a Zoomar Corporation, Glen Cove, N.Y., f/8, 102 cm focal length Cassegrainian telescope with an effective collection diameter of 10 cm. The monochromator slits were positioned at the prime focus of the telescope. The photomultiplier output was sent to an EG&G PAR Model 162 boxcar averager with a Model 164 gated integrator. Both the boxcar and the Tektronix model 453 oscilloscope were triggered by the synchronous output signal from the excimer laser. Traces of the photomultiplier signal and the gate output from the boxcar were simultaneously displayed on the oscilloscope. In this manner, one could easily adjust the aperture delay range on the boxcar such that the gated integration would overlap temporally with the molecular fluorescence LIDAR return signal. The boxcar output was then A/D converted and processed by the computer system.

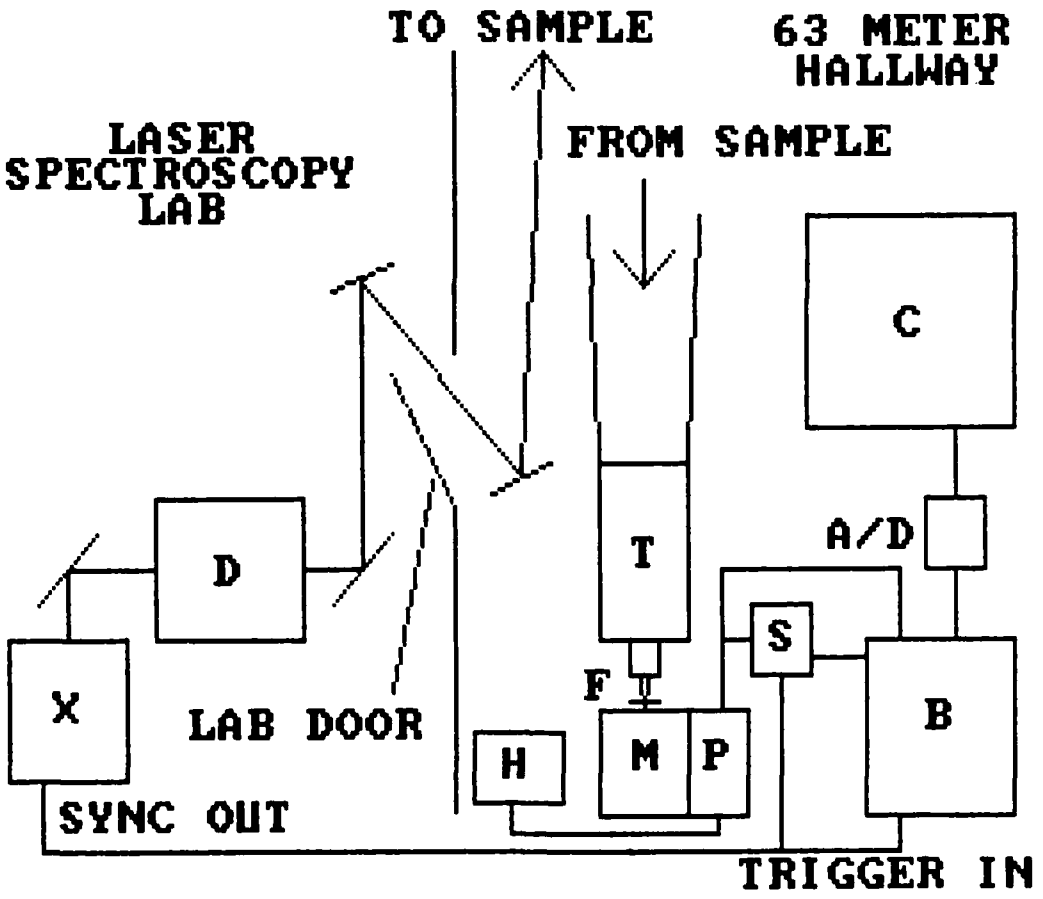

FIGURE 2. Remote Laser-Induced Fluorescence System. (X) excimer laser, (D) dye laser, (H) high voltage supply, (M) monochromator, (P) photomultiplier tube, (F) filter, (T) telescope (receiver), (S) oscilloscope, (B) boxcar averager, (A/D) analog/digital convertor, (C) computer.

Instruments model 229 power supply. Nominally, -1000 V were used for these experiments. Th photomultiplier output was next sent to a Quanta Ray DGA-1 dual gated amplifier, and its output was then analog to digitally (A/D) converted for processing with a Hewlett-Packard model HP9836A desktop computer system. The dual gated amplifier was operated with a 100-μs gate time and with a zero delay, relative to the trigger pulse.

The data acquisition was handled under the software control of a program titled AD_RTLG1 (A/D real time). To use the program, the operator first sets the monochromator manually to the emission wavelength to be monitored and enters information describing the PAH sample and the experimental conditions. The program then pauses, after displaying the axes and labels necessary for a fluorescence intensity versus real-time plot on the computer monitor screen. When all is ready, the program is continued by the operator and the data acquisition commences at time t = 0. The program plots the data and simultaneously displays the numeric values of the dependent and independent variables. For these experiments, each data point was the average of 20 samples taken by the A/D over a 0.5-second sampling period. As the program executes, the standard deviation is calculated and displayed, along with the point number, average intensity, and average time over which the samples were taken. A real-time interrupt function key is enabled during the processing to record the points of particular interest while the experiment is in progress (i.e., sample or wavelength changes, etc.). At the end of the data acquisition period, the operator can print the information on the experimental conditions and move a cursor through the data to examine and print any points of particular significance. Finally, the data set can be stored on disk for future use.

The AD_RTLG1 program can also be used to generate a plot of fluorescence intensity versus wavelength if one scans the monochromator manually. The operator can use the real-time interrupt key to record the time at which the monochromator passes specific wavelength settings during the scan.

REMOTE LIF SYSTEM

The LIF system used for the remote sensing experiments is shown in Figures 2 and 3. All of the components except the three dye laser beam-steering mirrors, the telescope, oscilloscope, and boxcar averager have been discussed in the previous section. The dye laser beam was steered out of the Laser Spectroscopy Laboratory and into the hallway using two 1-inch diameter, Newport Research Corporation, Fountain Valley, Calif., model 10QM20HM.45, 99.9% reflectivity, dielectrically coated 355 nm mirrors. These were followed by a final 2-inch diameter, 92% reflectivity front surface aluminum mirror.

A small fraction of the dye laser output was reflected off of a microscope slide and sent to a photodiode trigger for the dual gated amplifier. The laser beam was then sent through a 0.2 cm diameter iris before exciting the sample. Samples were contained in 1.0 cm path-length NSG Precision Cells quartz cuvettes which were mounted in a blackened aluminum cell block. This cell block had three 0.3 x 1.0 cm view-slots arranged in a T-configuration. The laser beam passed through two of the slots and the fluorescent emission was collected through the third at right angles to the beam path. The main purpose of the cell block was to reduce the amount of scattered laser light getting to the photodetection system.

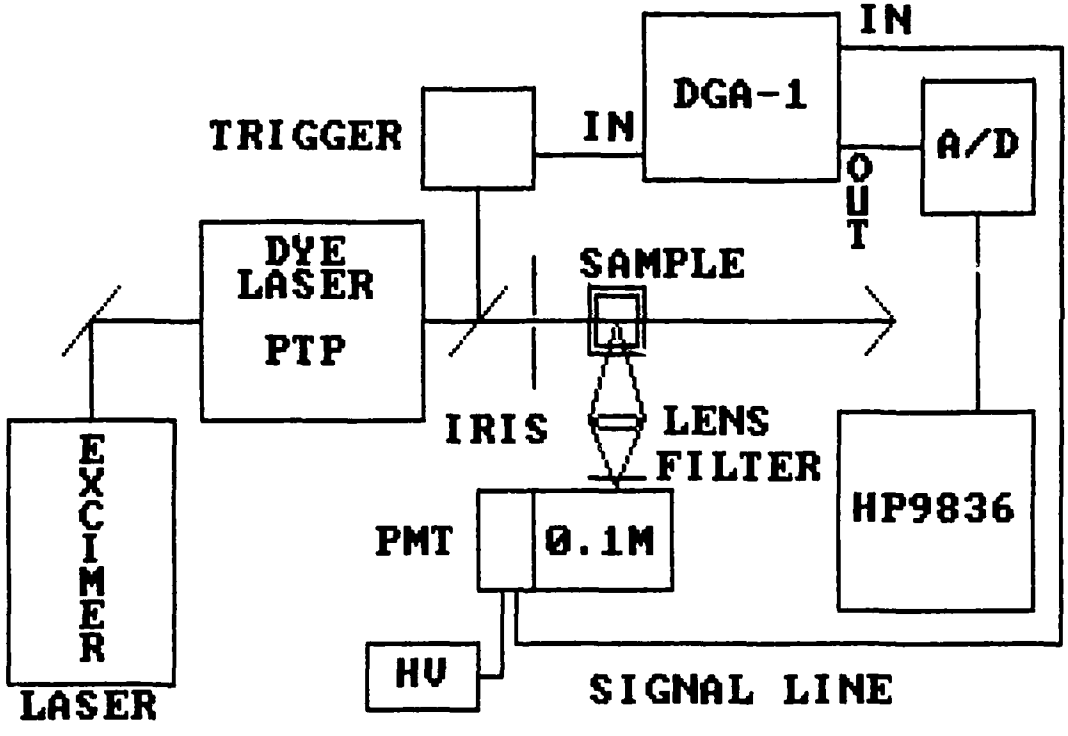

FIGURE 1. Laboratory Laser-Induced Fluorescence System.

The emitted fluorescence was collected with a quartz lens (f/2 efficiency), passed through a Corning 7380 glass filter, and focused onto the entrance slits of a Farrand Optical 0.1 m grating monochromator. The 0.05 x 0.5 cm slits produced a spectral bandpass of 2 nm. The dispersed fluorescent emission then struck the photocathode of an RCA 1P21 photomultiplier tube, mounted on the exit slit of the monochromator. The photomultiplier high voltage was supplied by a Pacific

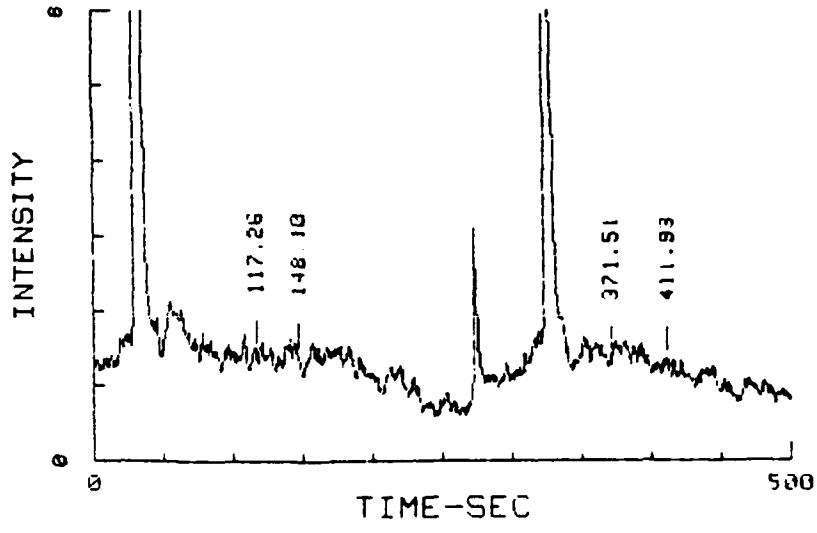

FIGURE 13. Two Successive Remote LIF Emission Spectra for a Pure Cyclohexane Blank. The sample location was 63 m from the receiver telescope and the excitation wavelength was 340 nm. The boxcar settings were as in Figure 11. Emission at 380 nm occurred at times of 117 and 371 seconds. Emission at 400 and 420 nm occurred at times of 148 and 441 seconds, respectively.

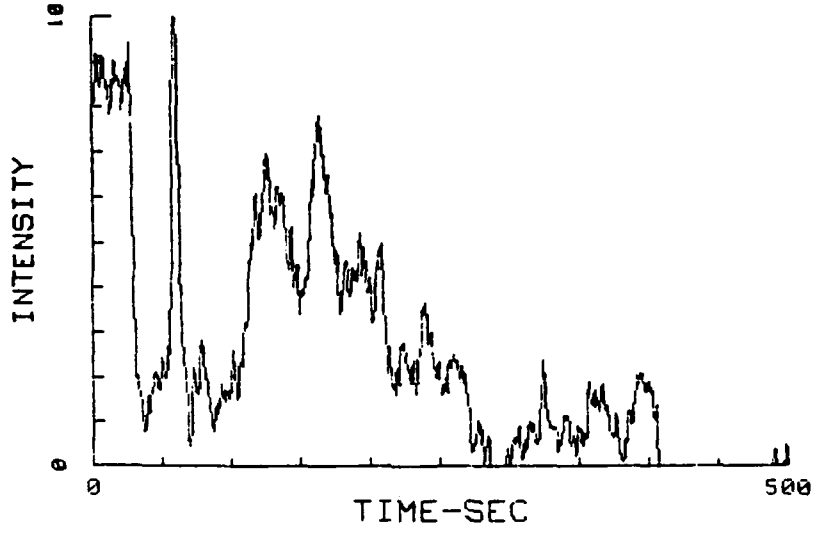

FIGURE 14. Remote LIF Emission Spectrum of the 2.1 ppm Solution of Anthracene in Cyclohexane. The sample location was 63 m from the receiver telescope and the excitation wavelength was 340 nm. The boxcar was terminated at 50 ohms, the gate time was 50 ns, and the aperture delay was set for 420 ns (round trip time for 63 m). The wavelength maxima were the same as in Figure 12. The drifting baseline is inherent to the boxcar when operated with a low duty cycle.

REMOTE DETECTION LEVEL PROJECTIONS

Armed with the results presented in the previous sections, a projection can now be made concerning feasibility of detecting gas-phase PAH concentrations in a PEP burn smoke plume on about a 1 ppm level at a range of 1 km. Many factors influence the potential sensitivity of a molecular fluorescence LIDAR system, and these will be discussed below, within the context of the system improvements and detection sensitivity estimates.

Since molecular fluorescence intensity is directly proportional to the excitation source intensity (neglecting saturation and higher-order effects), increasing the laser power will increase the returned LIF signal. Commercial flashlamp-pumped dye lasers, capable of outputting 100 mJ/pulse over the wavelength range from 262 to 375 nm are currently available (References 47 and 48). If one of these lasers were used for these experiments, a signal increase of a factor of 100 would be expected over the results reported here using 1 mJ/pulse at the sample. At a range of 1 km, the atmospheric transmission of the

340 nm laser excitation would be 58% of that at the 63 meter range (References 13 and 15). Similarly, the transmission factor for the LIF return signal at 400 nm would be 67%.*

In going from the solution to gas phase, the LIF volume backscattering coefficient for anthracene is affected by the changes in density, quantum yield, and atmospheric quenching. A measured factor of 592 was reported earlier in this publication. Including an additional factor of 2.1, because our measurements were made on a 2.1 ppm sample, one obtains an expected signal decrease of 1243 for the 1 km gas-phase experiments. However, the optical thickness of the solution sample was 0.5 cm and the optical thickness of the smoke plume from a large PEP burn could easily be 610 cm (20 ft). Therefore, this factor of 610/0.5 = 1220 approximately cancels the expected signal reduction in going from the solution to gas phase.

The effective receiver area, A_r, and the range, R, influence the magnitude of the LIF return signal through a factor of A_r/R^2, which determines the solid angle subtended by the receiver at range R. The use of a 50-cm telescope would provide a signal increase of 25, while the range factor would decrease the signal by 250. This results in an overall signal reduction factor of 10 for the solid angle considerations. This analysis assumes that the angle of divergence of the laser beam does not exceed the acceptance angle of the receiver, which poses no real problem. It also assumes that the laser beam is capable of penetrating the sampling range. This would probably require that the laser beam be steered away from the densest, particulate-laden portion of the smoke plume.

A more optically efficient telescope, photomultiplier tube, and monochromator would likely increase the signal by an additional factor of 3. As a matter of fact, the use of broadband filtering, rather than the monochromator could allow a much larger signal increase. Unfortunately, this would adversely affect the multicomponent mixture analysis selectivity. Nevertheless, PAH emission spectra are relatively broad (Reference 1), and the bandwidth of the emission monochromator could be increased from 2 to 20 nm without sacrificing much selectivity. This would result in a signal increase of a factor of 100.

*These conservative estimates were calculated from data taken where the meteorological range was only 13 km (8 mi). The meteorological range is defined as the farthest distance at which the human eye can see a large black object against the horizon sky. The visibility is often a good deal better than this in the high desert.

The combination of all the above factors would bring about a signal increase of 1166 over what was observed in Figure 12. Next, the noise and background increases must be considered for this "improved" system. The two major increases in noise and background would be brought about by the increased monochromator bandwidth and the increased receiver area. Factors of 100 and 25 would be expected for these system modifications. However, one could easily obtain a factor of 10 decrease in the receiver area contribution by decreasing the field-of-view of the telescope. These factors would result in an overall noise and background increase of 250.

From Figure 12, we take the signal to noise ratio to be a factor of 20. If this factor seems high, remember that the liquid sample had an optical thickness of 0.5 cm. Including the laser pulse width, the fluorescence lifetime of anthracene in cyclohexane (Reference 41) and the RC time constant of the boxcar in the analysis, the noise and background signal were being integrated for at least twice as long as the anthracene LIF signal, even in the 50 Ω termination experiment. At 1 mΩ, the black posterboard LIF also made a significant background contribution. Both of these situations would be improved upon in the optically thicker smoke plume.

Using the fact that the noise was approximately 5% of the signal in the solution-phase study, one obtains a total factor of 0.05 x 250 = 12.5 increase in noise and background for the gas-phase projections. This produces a final signal to noise ratio of 1166/12.5 = 93.3 for 1 ppm of gas-phase anthracene at a range of 1 km for the "improved" molecular fluorescence LIDAR system. This analysis assumes that the measurements would be done at night and does not include a number of other possible noise reductions. Examples of these would include improved electronics (good preamplifier and low capacitance leads), photomultiplier cooling to reduce dark current noise, and longer signal averaging (where the signal to noise ratio would improve in proportion to the square root of the number of pulses averaged). Lastly, it should be mentioned that the laser beam was observed to spatially fluctuate over the 7.5 cm diameter solution cells during the laboratory remote sensing experiments. This led to an additional source of noise that would not be as much of a problem for the extended target (smoke plume). Consideration of these factors would further improve the signal to noise ratio and make it easier to detect other PAHs that require bluer excitation (lower atmospheric transmission values) or have lower absorption cross sections or quantum yields than anthracene.

It would appear that the gas-phase detection of PAHs in concentrations on the order of 1 ppm at a range of 1 km is feasible. That is, detection *sensitivity* is not the major problem with the experiment. Detection *selectivity*, on the other hand, is a major problem and will be discussed more fully in the Conclusions and Recommendations section.

CONCLUSIONS AND RECOMMENDATIONS

CONCLUSIONS

A number of laboratory scale and remote LIF experiments have been performed on representative PAH molecules in order to test the feasibility of remotely detecting gas-phase PAHs produced in the combustion of PEP materials. Projections, based on measured gas- to solution-phase sensitivity factors and reasonable system improvements would indicate that 1 ppm PAH concentration levels could be detected at a range of 1 km. However, as has been previously discussed in the Background section, identification and quantification of the individual components in a complex PAH mixture introduces additional problems, some of which influence the detection sensitivity. For example, the selective identification and quantification of 10 or more PAHs in real time requires the rapid accumulation of large amounts of spectral data. Selective excitation over a wide range of wavelengths would be necessary to undertake this task. Although the 100 mJ/pulse commercial laser mentioned earlier is capable of being tuned from 262 to 370 nm, five dye changes and two second harmonic generation crystal changes are required to cover this wavelength range. Also, the output beams are dispersed through a prism, which means that the beam positions will be altered as the laser wavelength is tuned. The insertion of additional corrective optics would lower the power and adversely affect the sensitivity. The 100 mJ/pulse laser has a maximum pulse repetition frequency of 1 Hz. This affects the real-time nature of the data acquisition and minimizes the amount of signal averaging that could be accomplished in a reasonable time. Higher repetition frequency lasers are available, but the pulse energies are significantly lower (considering comparable economics and possible portability).

If the PAHs were condensed onto particulates, the spectral complexity problems would be magnified. In general, the emission spectra exhibit changes in going from the gas to solution to solid phase (Reference 1). It is also quite likely that solid-solid PAH interactions on the particulate matter would cause additional spectral shifts. Naturally, these shifts would depend upon which particular species were interacting. Under these conditions, the number of spectral "fingerprints" possible for a single PAH, interacting with many others, becomes overwhelming. These spectral shifts might also demand an expanded excitation tuning range, adding to the problems discussed above.

Nevertheless, some of these problems may be alleviated by concentrating on a small number of target compounds, perhaps even the more volatile PAHs, most likely to be in the gas phase. Many fluorescent materials are not likely to be good for the environment, even if they aren't PAHs. It may be valuable to at least know that something is out there, even if it cannot be completely characterized. A LIDAR-based

remote sensing system designed with the PAH detection problem in mind could also be used to monitor other environmentally hazardous materials, such as NO, NO_2, SO_2, O_3, etc. Ultimately, one has to weigh the cost of such a system (probably a few hundred thousand dollars) against the intermittent use of grab sampling techniques, with subsequent workup and analysis on a gas chromatography/mass spectrometry (GS/MS) system (which has its own associated set of problems).

RECOMMENDATIONS

Listed below are some recommendations for the basic components of a molecular fluorescence LIDAR-based remote PAH monitor.*

1. One, or multiple, high-powered pulse lasers (ca. 100 mJ/pulse) capable of tuning over 250 to 400 nm. The bandwidth can be several Angstroms, and the pulse width could be 250 ns (unless greater range resolution is desired). The maximum pulse repetition frequency should be as high as possible without sacrificing peak power. The use of multiple lasers would reduce the number of dye and second harmonic crystal changes required to cover the wavelength range.

2. A reflective telescope of at least 50 cm diameter. The field of view should be as low as possible in order to reject unwanted background contributions.

3. A low resolution (ca. 10 to 20 nm) monochromator capable of dispersing light over the 300 to 600 nm range. It should be able to operate with a diode array detection system.

4. A cooled, gated, image intensified diode array detection system. The gating capability will allow the temporal discrimination of unwanted background radiation and also allow some discrimination among the PAHs themselves. The image intensification is necessary for sensitivity and UV detection. This device will allow the collection of single-shot spectra in addition to a signal averaging capability (References 30 through 33).

5. One or multiple computer systems for the complete automation of all of the above including the wavelength tuning of the laser(s). The design considerations would incorporate rapid response, sophisticated experimental control, and the elimination of tedious, inefficient manual operations.

*Some of these considerations have been discussed in the section on Remote Detection Level Projections.

REFERENCES

1. Naval Weapons Center. *The Design and Operation of a Real-Time Polynuclear Aromatic Hydrocarbon (PAH) Monitor for the Analysis of Combustion Products Formed in the Incineration of Navy Colored Smoke Compositions*, by R. T. Loda, Research Department. China Lake, Calif., NWC, August 1984. 134 pp. (NWC TP 6525, publication UNCLASSIFIED.)

2. ------. *Real-Time Fluorescence Analysis of the Controlled Incineration of Army Colored Smoke Compositions*, by R. T. Loda and T. P. Parr, Research Department. China Lake, Calif., NWC, November 1984, 80 pp. (in process). (NWC TP 6559, publication UNCLASSIFIED.)

3. Naval Weapons Support Center. *Controlled Incineration of Navy Colored Smoke Compositions*, by Applied Sciences Department. Crane, Ind., NWSC, July 1978. 81 pp. (NWSC/CR/RDTR-86, publication UNCLASSIFIED.)

4. A. Chin and L. Borer. "Identification of Combustion Products from Colored Smokes Containing Organic Dyes," *Prop., Explo., Pyrotech.*, Vol. 8 (August 1983), pp. 112-118.

5. Naval Weapons Center. *Pollution Abatement Research and Development July-September 1982*, by Research Department. China Lake, Calif., NWC, November 1982. 40 pp. (NWC TP 6407, publication UNCLASSIFIED.)

6. ------. *Pollution Abatement Research and Development October-December 1982*, by Research Department. China Lake, Calif., NWC, February 1983. 44 pp. (NWC TP 6431, publication UNCLASSIFIED.)

7. ------. *Pollution Abatement Research and Development January-March 1983*, by Research Department. China Lake, Calif., NWC, May 1983. 56 pp. (NWC TP 6446, publication UNCLASSIFIED.)

8. ------. *Pollution Abatement Research and Development April-June 1983*, by Research Department. China Lake, Calif., NWC, October 1983. 66 pp. (NWC TP 6477, publication UNCLASSIFIED.)

9. ------. *Pollution Abatement Research and Development July-September 1983*, by Research Department. China Lake, Calif., NWC, December 1983. 46 pp. (NWC TP 6496, publication UNCLASSIFIED.)

10. ------. *Pollution Abatement Research and Development October-December 1983*, by Research Department. China Lake, Calif., NWC, February 1984. 28 pp. (NWC TP 6520, publication UNCLASSIFIED.)

11. Naval Weapons Center. *Pollution Abatement Research and Development January-March 1984*, by Research Department. China Lake, Calif., NWC, May 1984. 28 pp. (NWC TP 6547, publication UNCLASSIFIED.)

12. ------. *Pollution Abatement Research and Development April-June 1984*, by Research Department. China Lake, Calif., NWC, August 1984. 28 pp. (NWC TP 6574, publication UNCLASSIFIED.)

13. *Laser Monitoring of the Atmosphere*, E. D. Hinkley, ed. Berlin, Germany, Springer-Verlag, 1976, and references therein.

14. *Surveillance of Environmental Pollution and Resources by Electromagnetic Waves*. Terje Lund, ed. Dordrecht, Holland, D. Reidel Publishing Co., 1978, and references therein.

15. *Remote Sensing: Optics and Optical Systems*, Philip N. Slater. Massachusetts, Addison-Wesley, 1980.

16. *Optical and Laser Remote Sensing*, D. K. Killinger and A. Mooradian, ed. Berlin, Germany, Springer-Verlag, 1983, and references therein.

17. *Polynuclear Aromatic Hydrocarbons: Chemistry and Biological Effects*, A. Bjorseth and A. J. Dennis, eds. Ohio, Battelle Press, 1980. 1097 pp., and references therein.

18. *Chemical Analysis and Biological Fate: Polynuclear Aromatic Hydrocarbons*, M. Cooke and A. J. Dennis, eds. Ohio, Battelle Press, 1981. 800 pp., and references therein.

19. B. L. Sharp. "Laser Remote Sensing of Atmospheric Pollutants," *Chem. in Brit*, May 1982, pp. 342-347.

20. K. Fredriksson, and others. "Mobile LIDAR System for Environmental Probing," *Appl. Opt.*, Vol. 20, No. 24 (December 1981), pp. 4181-4189.

21. E. V. Browell. "LIDAR Measurements of Tropospheric Gases," *Opt. Eng.*, Vol. 21, No. 1 (January/February 1982), pp. 128-132.

22. O. T. Troy. "Lasers Close in on Pollution," *Photonics Spectra*, July 1984, pp. 66-68.

23. G. A. Capelle and L. A. Franks. "Laboratory Evaluation of Two Laser Fluorosensor Systems," *Appl. Opt.*, Vol. 18, No. 21 (November 1979), pp. 3579-3586.

24. R. A. O'Neil, L. Buja-Bijunas and D. M. Rayner. "Field Performance of a Laser Fluorosensor for the Detection of Oil Spills," *Appl. Opt.*, Vol. 19, No. 6 (March 1980), pp. 863-870.

25. R. Dick, S. M. Till and R. A. O'Neil. "Remote Sensing of PAH by Laser Induced Fluorescence," in *Chemical Analysis and Biological Fate: Polynuclear Aromatic Hydrocarbons*, ed. by M. Cooke and A. J. Dennis. Ohio, Battelle Press, 1981. Pp. 731-740.

26. G. P. Quigley. "The Synchronous Detection of Laser-Induced Fluorescence," in *Remote Detection of Hazardous Materials (Propellants and Related Items)*, ed. by J. A. E. Hannum. Chemical Propulsion Information Agency Workshop Proceedings. Maryland, Johns Hopkins, July 1982. Pp. 323-338. Paper UNCLASSIFIED.

27. P. Burlamacchi and others. "Performance Evaluation of UV Sources for LIDAR Fluorosensing of Oil Films," *Appl. Opt.*, Vol. 22, No. 1 (January 1983), pp. 48-53.

28. G. P. Quigley. "Laser Detection of Hazardous Molecules," *Laser Focus* (March 1983), pp. 21-22.

29. G. A. Capelle, L. A. Franks and D. A. Jessup. "Aerial Testing of a KrF Laser-Based Fluorosensor," *Appl. Opt.*, Vol. 22, No. 21 (November 1983), pp. 3382-3387.

30. G. D. Christian, J. B. Callis, and E. R. Davidson. "Array Detectors and Excitation-Emission Matrices in Multicomponent Analysis," in *Modern Fluorescence Spectroscopy*, ed. by E. L. Wehry. New York, Plenum Press, 1981. Vol. 4, Chap. 4, pp. 111-165.

31. I. M. Warner and L. B. McGowan. "Recent Advances in Multicomponent Fluorescence Analysis," in *CRC Critical Reviews in Analytical Chemistry*, February 1982, pp. 115-222.

32. M. P. Fogarty and I. M. Warner. "Ratio Method for Fluorescence Spectral Deconvolution," *Anal. Chem.*, Vol. 53, No. 2 (February 1981), pp. 259-265.

33. M. P. Fogarty, C.-N. Ho and I. M. Warner. "Data Handling in Fluorescence Spectrometry," in *Optical Radiation Measurements*, ed. by. K. D. Mielenz. New York, Academic Press, Vol. 3, 1982. Pp. 249-314.

34. A. W. Tucker, M. Birnbaum, and C. L. Fincher. "Fluorescence of Fly Ash Samples: Implications for In Situ and Remote Detection," *J. Lumin.*, Vol. 9 (1974), pp. 1-8.

35. A. H. Miguel and others. "Apparatus for Vapor-Phase Adsorption of Polycyclic Organic Matter onto Particulate Surfaces," *Envir. Sci. and Tech.*, Vol. 13, No. 10 (October 1979), pp. 1229-1232.

36. G. Prado and others. "Formation of Polycyclic Aromatic Hydrocarbons in Premixed Flames. Chemical Analysis and Mutagenicity," in *Chemical Analysis and Biological Fate: Polynuclear Aromatic Hydrocarbons*, M. Cooke and A. J. Dennis eds. Ohio, Battelle Press, 1981. Pp. 189-198.

37. W. H. Griest and J. E. Caton. "Studies of the Interaction of Polycyclic Aromatic Hydrocarbons with Fly Ash," in *Chemical Analysis and Biological Fate: Polynuclear Aromatic Hydrocarbons*, ed. by M. Cooke and A. J. Dennis. Ohio, Battelle Press, 1981. Pp. 719-730.

38. F. Beretta, A. Cavaliere, and A. D'Alessio. "Laser Excited Fluorescence Measurements in Spray Oil Flames for the Detection of Polycyclic Aromatic Hydrocarbons and Soot," *Comb. Sci. and Tech.*, Vol. 27 (1982), pp. 113-122.

39. *CRC Handbook of Chemistry and Physics*, R. C. Weast and M. J. Astle, eds. Florida, CRC Press, 1981-1982.

40. R. Kaminski, R. Obenauf, and F. Purcell. "Focus on Fluorescence," *The Spex Speaker*, Vol. 27, No. 1 (March 1982), pp. 1-9.

41. I. B. Berlman. *Handbook of Fluorescence Spectra of Aromatic Molecules*. New York, Academic Press, 1971.

42. J. Timmermans. *Physico-Chemical Constants of Pure Organic Compounds*. New York, Elsevier, 1965, Volume 2.

43. H. P. Burchfield, R. J. Wheeler, and J. B. Bernos. "Fluorescence Detector for Analysis of Polynuclear Arenes by Gas Chromatography," *Anal. Chem.*, Vol. 43, No. 14 (December 1971), pp. 1976-1981.

44. D. F. Freed and L. R. Faulkner. "Characterization of Gas Chromatographic Effluents via Scanning Fluorescence Spectrometry," *Anal. Chem.*, Vol. 44, No. 7 (June 1972), pp. 1194-1198.

45. J. W. Robinson and J. P. Goodbread. "A Selective Gas Chromatographic Detector for Polynuclear Aromatics Based on Ultraviolet Fluorescence," *Anal. Chim. Acta*, Vol. 66 (1973), pp. 239-244.

46. R. P. Cooney and J. D. Winefordner. "Instrumental Effects on Limits of Detection in Gas Phase Fluorescence Detection of Gas Chromatographic Effluents," *Anal. Chem.*, Vol. 49, No. 7 (June 1977), pp. 1057-1060.

47. J. Hecht. "Comparing Types of Dye Lasers," *Lasers and Appl.* (July 1984), pp. 53-61.

48. Lasers and Applications Staff. "Pulsed and CW Dye Laser Matrix: A Survey of Specifications for Commercial Dye Lasers," *Lasers and Appl.* (July 1984), pp. 63-67.

INITIAL DISTRIBUTION

9 Naval Air Systems Command
- AIR-03B, H. Andrews (1)
- AIR-03D, G. Heiche (1)
- AIR-310G, R. Shumaker (1)
- AIR-320R, H. Rosenwasser (1)
- AIR-330 (1)
- AIR-35 (1)
- AIR-536A1 (1)
- AIR-7226 (2)

5 Chief of Naval Operations
- OP-225 (1)
- OP-354 (1)
- OP-506 (1)
- OP-982E (1)
- OP-982F (1)

1 Chief of Naval Material (MAT-08)

5 Chief of Naval Research, Arlington
- ONR-440 (1)
- ONR-443 (1)
- ONR-460 (1)
- ONR-470 (1)
- ONR-472 (1)

3 Naval Facilities Engineering Command, Alexandria
- Code 032, S. Hurley (1)
- Code 112 (1)
- Code 54 (1)

7 Naval Sea Systems Command
- SEA-04E (1)
- SEA-05R1 (1)
- SEA-05R14 (1)
- SEA-05R16 (1)
- SEA-09B312 (2)
- SEA-62R32 (1)

1 Commander in Chief, U.S. Pacific Fleet (Code 325)

1 Commander, Third Fleet, Pearl Harbor

1 Commander, Seventh Fleet, San Francisco

2 Naval Academy, Annapolis (Director of Research)

2 Naval Air Development Center, Warminster
- Library (1)

1 Naval Air Propulsion Center, Trenton (PE-71, A. F. Klarman)

1 Naval Energy and Environmental Support Activity, Port Hueneme

3 Naval Ocean Systems Center, San Diego
- Code 521, M. H. Salazar (1)
- Code 522
  - S. Yamamoto (1)
  - A. Zirino (1)

2 Naval Ordnance Station, Indian Head
- Code E, Pollution Abatement Program Manager (1)
- Technical Library (1)

3 Naval Research Laboratory
- Code 4300 (1)
- Code 6100 (1)
- Library (1)

3 Naval Ship Weapon Systems Engineering Station, Port Hueneme
Code 5711, Repository (2)
Code 5712 (1)
2 Naval Surface Weapons Center, Dahlgren
G-51 (1)
Technical Library (1)
5 Naval Surface Weapons Center, White Oak Laboratory, Silver Spring
Code R11 (2)
Code R16, J. Hoffsommer (1)
Code R17 (1)
Code R141, G. Young (1)
1 Naval War College, Newport
6 Naval Weapons Support Center, Crane
Code 5025, D. Burch (1)
Code 50C, B. E. Douda (1)
Code 505, J. E. Short (1)
NAPEC (1)
R&E Library (2)
4 Office of Naval Technology, Arlington
MAT-0716 (1)
MAT-072 (1)
MAT-0723 (1)
MAT-0724 (1)
1 Army Armament Munitions & Chemical Command, Rock Island (AMSMC-DSM-D, D. Sevey)
1 Army Environmental Hygiene Agency, Aberdeen Proving Ground (HSHB-EA-A)
1 Army Medical Bioengineering Research and Development Laboratory, Fort Dietrick (J. Barkeley)
1 Army Toxic and Hazardous Materials Agency, Aberdeen Proving Ground (DRXTH-TE-D)
3 Air Force Systems Command, Andrews Air Force Base
DLFP (1)
DLWA (1)
SDZ (1)
1 Air Force Armament Division, Eglin Air Force Base (AFATL/DLJW)
1 Air Force Inteiligence Service, Bolling Air Force Base (AFIS/INTAW, Maj. R. Lecklider)
12 Defense Technical Information Center
1 Los Alamos National Laboratory, Los Alamos, NM (R. Koenig, MS E517)
1 Michigan State University, East Lansing, MI (Chemistry Department, E. D. Erickson)
3 The Johns Hopkins University, Applied Physics Laboratory, Chemical Propulsion Information Agency, Laurel, MD
T. W. Christian (2)
J. Hannum (1)

END

FILMED

5-85

DTIC